PHYSICAL REVIEW C VOLUME 12, NUMBER 4 OCTOBER 1975

# Radiative decay of the second excited state of $^{12}C$

H.-B. Mak,* H. C. Evans,* and G. T. Ewan*
*Queen's University, Kingston, Ontario, Canada*

A. B. McDonald and T. K. Alexander
*Atomic Energy of Canada Limited, Chalk River Nuclear Laboratories, Chalk River, Ontario, Canada KOJ 1JO*

(Received 13 May 1975)

The branching ratio $\Gamma_{rad}/\Gamma$ for the electromagnetic decay of the 7.655 MeV second excited state of $^{12}C$ has been measured by detecting the $^{12}C$ (0.0 MeV) recoils in coincidence with $\alpha$ particles from the $^{13}C(^3He,\alpha_2)^{12}C$ (7.655 MeV) reaction at $E_{^3He}=4.00$ MeV. Coincidence events were identified by means of time-of-flight, energy, and kinematic constraints. Thus, of all the $^{12}C$ nuclei formed in the second excited state, only those decaying to the $^{12}C$ ground state by either $\gamma$-ray or positron-electron pair emission were selected. Hence the experiment provides a direct measurement of $\Gamma_{rad}/\Gamma$, where $\Gamma_{rad}=\Gamma_\gamma+\Gamma_{e\pm}$, and gives $\Gamma_{rad}/\Gamma=(4.15\pm0.34)\times10^{-4}$, which is in good agreement with other recent measurements, and suggests that the previously accepted value of $\Gamma_{rad}/\Gamma=(2.9\pm0.3)\times10^{-4}$ may be too low. The significance of this result is discussed with respect to helium burning rates in stars.

[NUCLEAR REACTIONS $^{13}C(^3He,\alpha)$, $E=4.0$ MeV; measured $\alpha$-$^{12}C$ coin. $^{12}C$ level deduced $\Gamma_{rad}/\Gamma$. Enriched target.]

## I. INTRODUCTION

Recently a number of nuclear physics experiments have been focused on the critical parameters defining the rates of helium burning in stars.[1-3] This paper describes a measurement of the branching ratio for radiative decay of the 7.655 MeV $0^+$ level of $^{12}C$, which is the dominant resonance in the process $3\alpha\to{}^{12}C$. This process is thought to be the means for producing heavier nuclei from light nuclei ($A\leq4$) in quiescent stellar nuclear synthesis, bypassing the mass numbers 5 and 8 for which no stable nucleus exists.

Helium burning arises after the completion of hydrogen burning within the core of a star. When the energy generation from the conversion of hydrogen to helium is ended, the core contracts, and the conversion of gravitational energy into kinetic energy increases the temperature of the central region of the star. The contraction of the core is interrupted only if the temperature is high enough to ignite the helium fuel, or if the star can be stabilized as degenerated matter and ceases to radiate.

Opik[4] and Salpeter[5] suggested that when the helium core reached a temperature of $T\sim10^8$ K and a density of $\rho\sim10^5$ g/cm$^3$, fusion of helium gas into $^{12}C$ could take place through the two-step process

$$^4He+{}^4He\rightleftharpoons{}^8Be\ , \tag{1}$$

and

$$^4He+{}^8Be\rightleftharpoons{}^{12}C^*\ . \tag{2}$$

On the basis of reaction rates and the relative abundances of $^4He$ and $^{12}C$, Hoyle pointed out that reaction (2) had to go through a resonance in $^{12}C$. A level with an excitation energy of approximately 7.7 MeV was subsequently located,[6] and its spin and parity were determined[7] to be $0^+$. Assuming a two-step process through a sharp resonance in $^{12}C$, the equilibrium concentration of $^{12}C^*$ is given by[8]

$$N(^{12}C^*)=N_\alpha{}^3f_1f_2\frac{h^6(3)^{3/2}}{(2\pi M_\alpha kT)^3}\exp\left(-\frac{Q}{kT}\right)\ , \tag{3}$$

where $N_\alpha$ is the concentration of $^4He$; $f_1$ and $f_2$ are the electronic-screening factors for successive reactions 1 and 2; $Q$ is the mass difference between the resonance in $^{12}C$ and the sum of three $\alpha$ particles; $M_\alpha$ is the mass of the $\alpha$ particle; $h$ is Planck's constant and $k$ is the Boltzmann constant. Reactions (1) and (2), however, are not in true equilibrium because of a small leakage of $^{12}C^*$ to $^{12}C$ (0.0 MeV) by electromagnetic decay. If all the $^{12}C$ (0.0 MeV) is assumed to be generated through the formation of the second excited state, then the rate of producing $^{12}C$ nuclei from three helium particles is given by

$$R=N_\alpha{}^3f_1f_2\frac{h^5(3)^{3/2}\Gamma_{rad}}{(2\pi)^2(M_\alpha kT)^3}\exp\left(-\frac{Q}{kT}\right)\ . \tag{4}$$

For a given temperature and density, the rate depends critically on $Q$ and $\Gamma_{rad}$. A direct measurement of the $Q$ value has been done recently by Barnes and Nichols.[1] Many experiments[2] were carried out to measure the excitation energy of the second excited state in $^{12}C$, and the $Q$ value was deduced from the excitation energy and the mass difference between the $^{12}C$ ground state and three $\alpha$ particles. The weighted average of these measurements gives $Q = 380.1 \pm 1.0$ keV, and the 1 keV uncertainty in $Q$ introduces a 11.6% uncertainty in the calculated triple $\alpha$ rate at $T = 10^8$ K.

A number of experiments[9] were carried out to measure the ratio $\Gamma_{rad}/\Gamma$ from which $\Gamma_{rad}$ can be derived through the relationship

$$\Gamma_{rad} = \frac{\Gamma_{rad}}{\Gamma} \frac{\Gamma}{\Gamma_{e\pm}} \Gamma_{e\pm} .$$

The positron-electron pair emission width $\Gamma_{e\pm}$ was calculated from electron inelastic scattering data.[10] The branching ratio $\Gamma_{e\pm}/\Gamma$ was measured by Alburger[11] and Obst, Grandy, and Weil.[12] The value $\Gamma_{rad}/\Gamma = (4.20 \pm 0.22)\times 10^{-4}$ recently published by Chamberlin *et al.*[3] is in serious disagreement with the older accepted value[13] of $\Gamma_{rad}/\Gamma = (2.9 \pm 0.3)\times 10^{-4}$. A number of attempts are being made to try to resolve this discrepancy.[14] Our measurement of this branching ratio gives $\Gamma_{rad}/\Gamma = (4.15 \pm 0.34)\times 10^{-4}$, confirming the result of Chamberlin *et al.*[3] A preliminary description of the present experiment has been given previously.[15]

## II. EXPERIMENTAL PROCEDURE

The branching ratio $\Gamma_{rad}/\Gamma$ for the electromagnetic decay of the 7.655 MeV second excited state of $^{12}C$ was measured by detecting the $^{12}C$ (0.0 MeV) recoils in coincidence with $\alpha$ particles from the $^{13}C(^3He, \alpha_2)^{12}C$ (7.655 MeV) reaction at $E_{^3He} = 4.00$ MeV.

The singly charged $^3He$ beam was generated by the 4 MeV Van de Graaff accelerator at Queen's University, and the beam current was maintained at approximately 0.7 $\mu$A throughout the experiment. The $^{13}C$ foils (enriched to ~90%) were approximately 15 $\mu g/cm^2$ thick and were supplied by the Commercial Products Division of Atomic Energy of Canada Limited. The foils were produced by evaporating enriched $^{13}C$ onto glass slides coated with approximately 15 $\mu g/cm^2$ of $BaCl_2$ as parting agent. They were stored in an argon atmosphere to reduce the absorption of $^{14}N$, and exposure to air was kept to a minimum while the targets were being prepared. They were mounted in double thickness to produce 30 $\mu g/cm^2$ thick self-supporting targets. The usuable target area was about 0.95 cm in diameter, allowing the same target to be bombarded on several spots. The bombarded spot was changed every four hours.

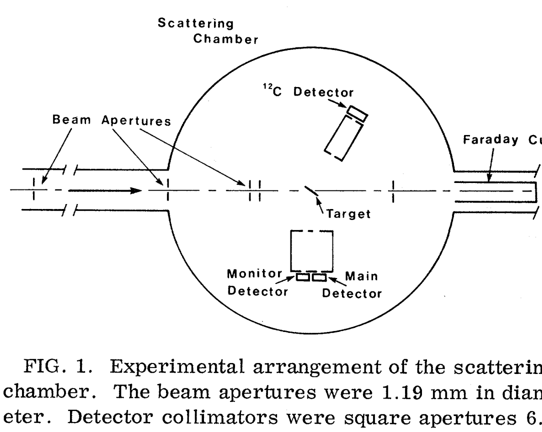


FIG. 1. Experimental arrangement of the scattering chamber. The beam apertures were 1.19 mm in diameter. Detector collimators were square apertures 6.35 mm× 6.35 mm in size with round corners.

As a preliminary measurement, excitation functions and angular distributions of the $^{13}C(^3He, \alpha_2)$-$^{12}C_2$ reaction were measured from 3 to 4 MeV. The angular distributions have maxima at $\theta_\alpha \simeq 90°$, and the maximum value of the differential cross section increases with beam energy. At 4 MeV, the maximum energy available, the differential cross sections at the $\alpha$ detector angles used are 0.20 mb/sr at $\theta_\alpha = 85.3°$ and 0.16 mb/sr at $\theta_\alpha = 100.6°$. At these angles, the $\alpha_2$ energies are 8.44 MeV and 7.78 MeV; the $^{12}C_2$ recoil angles are 62.7 and 50.6°; and the $^{12}C_2$ recoil energies are 3.56 and 4.18 MeV, respectively.

Figure 1 shows the experimental arrangement of the scattering chamber. The beam was collimated by three collinear apertures 1.19 mm in diameter situated at distances 67.3, 26.7, and 12.7 cm from the target. Another aperture, 1.6 mm in diameter, was placed at a distance of 8.3 cm from the target to remove $^3He$ scattered from the edges of the collimators upstream. The target was placed at an angle of 45° to the beam. A collimator with a 3.2 mm diameter hole was located in front of the Faraday cup. The current striking this collimator as well as that collected by the antiscattering collimator was minimized and monitored throughout the experiment as a check on the stability of the beam position.

Both the $^{12}C$ detector and the $\alpha$ detector (labeled Main Detector in Fig. 1) were 100 $\mu$m thick 50 $mm^2$ ruggedized silicon surface barrier detectors. The $^{12}C$ detector was mounted on a movable plate at the bottom of the chamber, and the $\alpha$ detector was mounted on a movable arm from the top of the chamber. Both detectors were at a distance of 10.16 cm from the target, and were collimated by square apertures 6.35 mm×6.35 mm in area. The corners of the apertures were rounded off with a radius of 0.79 mm, and the detectors were mounted such that only the active part of the detectors could be seen through the collimators. The angle subtended by the collimators was 3.59°. Assuming a beam diameter of 1.19 mm, the extreme ends of the beam spot at the target would subtend an angle of 0.7° at the center of the main $\alpha$ detector.

To locate the position of the $^{12}C$ detector relative to the reaction plane defined by the main $\alpha$ detector and the beam, thin lucite pieces were mounted on the detector holders and were swung into the beam path at 0 and 180°, respectively, producing well-defined beam marks. The two planes defined by the rotation of the detectors were known to be parallel to each other from the geometry of the target chamber so this test served to define the heights of these planes relative to the beam. It was found that the main $\alpha$ detector plane was 0.635 mm above the beam line and the $^{12}C$ detector plane was 0.381 mm above the beam line. The average $^{12}C$ recoil direction, as defined by the positions of the beam spot and the $\alpha$ detector, would result in $^{12}C$ recoils striking the $^{12}C$ detector 1.016 mm below the center. This was taken into account in calculating detection efficiences.

The energy loss in the target was about 23 keV for the incident $^3He$ beam and 18 keV for the $\alpha$ particles. The kinematic spread of the $\alpha_2$ particles, including the finite size of the beam spot, was about 184 keV. The corresponding kinematic spread in the $^{12}C_2$ recoils was about 176 keV. The energy loss in the target was about 240 keV for the $^{12}C_2$ recoils. Emission of $\gamma$ rays could change the $^{12}C_2$ recoil energy by as much as 190 keV and the $^{12}C_1$ recoil energy by 130 keV. Allowing for small differences in the kinematic spreads and energy losses, the over-all energy resolution was estimated to be approximately 160 keV for $^{12}C_1$ recoils and 240 keV for $^{12}C_2$ recoils. While in most cases the experimental resolution was found to be as expected, the $^{12}C_1$ peak was somewhat poorer in resolution, having the same width as the $^{12}C_2$ peak (approximately 250 keV).

A third 100 $\mu$m thick 50 mm$^2$ ruggedized surface barrier detector (labeled Monitor Detector) was placed beside the main $\alpha$ detector. This detector was collimated by an aperture similar to those used in the other detectors, and was used in a coincidence system identical to the main detector. The detector angle (9.4° from the main detector) was chosen so that the efficiency for detection of $\alpha_0$-$^{12}C_0$ coincidences was very sensitive to devia-

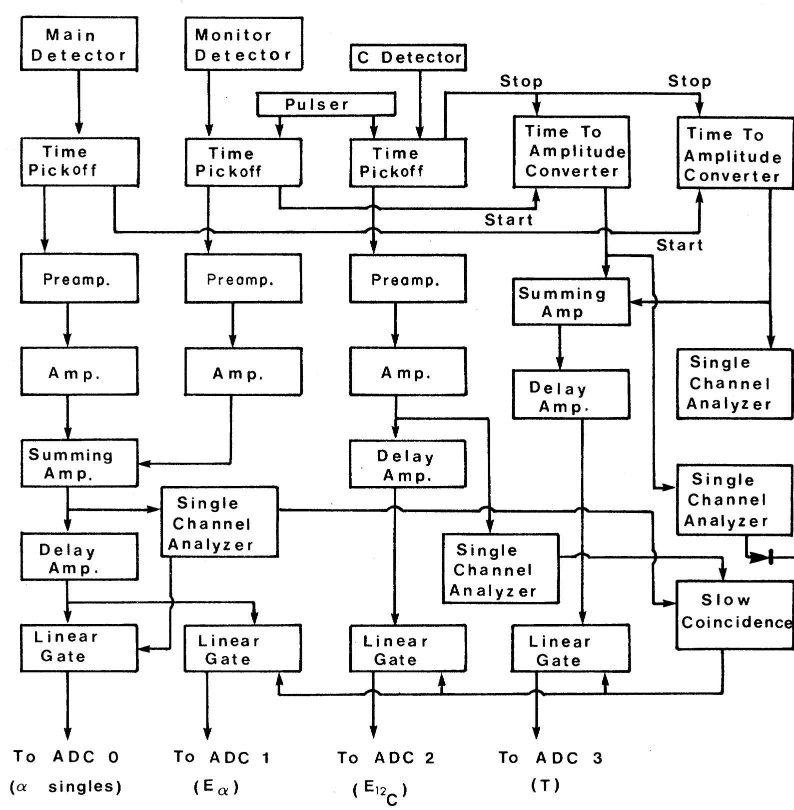


FIG. 2. Block diagram of the electronic circuitry used in the coincidence measurement. Conventional slow and fast electronics were used. Singles events were analyzed by ADC 0 and stored in a PDP-11 computer. Coincidence events were analyzed by ADC 1, ADC 2, and ADC 3 and stored on tape and in a PDP-15 computer.

tion in beam position. This parallel detection system was used to obtain coincidence dead-time corrections and to monitor the stability of the system.

Figure 2 shows a block diagram of the electronics used in the coincidence measurements. Time-pickoff units provided fast timing signals. With different delays for signals from the $\alpha$ and the monitor detectors, the time spectra were shifted such that the time-to-amplitude converter (TAC) peak between $^{12}C$ events and main events was in the time range $100 \geq T \geq 65$ nsec, and coincidences between $^{12}C$ events and monitor events were in the time range $60 \geq T \geq 15$ nsec. The time resolution of the system was about 0.7 nsec, but over periods of days small time shifts resulted in poorer resolution, and the over-all time resolution was about 1.5 nsec. The outputs of the TAC's were inspected by separate single-channel analyzers ($T$ single channel analyzers) and then summed. The linear main signals and monitor signals were summed and inspected by another single channel analyzer ($E_\alpha$ single channel analyzer). The gain of the main detector system was set slightly higher than that of the monitor detector system. For singles energy spectra, the main and monitor events, gated by the $E_\alpha$ single channel analyzer, were analyzed by and stored in a PDP-11 computer. The threshold of the $E_\alpha$ single channel analyzer was set at 4.0 MeV to reduce the dead time of the computer. The linear $^{12}C$ signals were inspected by a fourth single channel analyzer ($E_C$ single channel analyzer) which was set to accept events with energy higher than 0.65 MeV. A slow triple coincidence between the outputs of the $E_\alpha$ and $E_C$ single channel analyzers and the mixed outputs of the $T$ single channel analyzers was used to gate the time and the energy signals. Coincidence events were characterized by main or monitor energy ($E_\alpha$), $^{12}C$ energy ($E_C$), and time-of-flight difference ($T$), which were written on magnetic tapes in related address mode by a PDP-15 computer. The data were sorted on-line into spectra for monitoring purposes. Final data analysis was performed on the PDP-10 computer at Chalk River.

The relative counting loss between the singles system and the coincidence system was monitored by means of a pulser connected to the $C$ detector system and the monitor detector system. The pulser was triggered externally by pulses obtained from a neutron detector. The rate was adjusted by placing the neutron detector at different distances from the target. Since more than 75% of the neutrons were produced from the target [probably by the $^{13}C(^3He,n)^{14}O$ reaction], the pulser counts should be random in time and the rate should be approximately proportional to the $^{13}C(^3He,\alpha)$ rate.

The count rate in the $^{12}C$ detector was about 18 000 counts per second for events above an energy of 300 keV. There was an additional high rate at lower energies mainly from low energy $^{13}C$ recoils from elastic scattering. The over-all

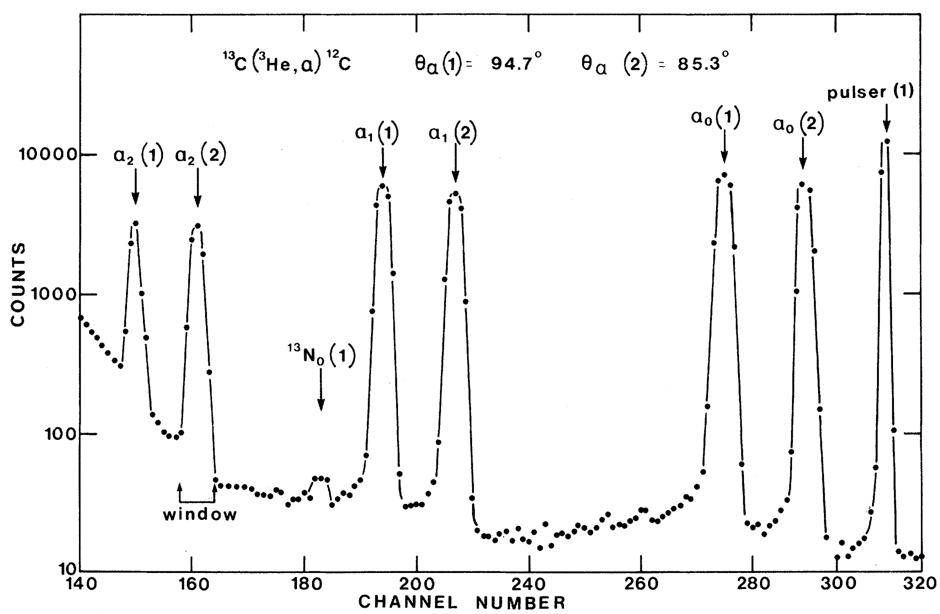


FIG. 3. Partial singles, main plus monitor detector spectrum at $\theta_\alpha = 85.3°$ (monitor detector at 94.7°). Peaks labeled with (1) are from the monitor system and those labeled with (2) are from the main system.

effect of this rate on the peaks of interest was evaluated from the effect on the pulser peak. About 3% of the pulser counts were thrown out of the sharp peak as a result of pileup. Most of the pileup events were contained in a flat platform extending about 250 keV on either side of the peak. The peaks of interest from $^{12}$C recoils were about 250 keV wide so that the percentage loss for them was less than 3%, and was calculated from the distortion of the pulser peak.

The main and monitor detectors had counting rates of about 8 000 per second. In this case pileup was found to be less, because of the much lower energy of $^{13}$C recoils near 90°. The remaining pileup could be neglected since it affected peaks similarly in singles and coincidence spectra. Dead-time corrections were about 4% for the singles spectra and negligible for the coincidence spectra.

## III. DATA AND ANALYSIS

Since the coincidence rate was low, over 144 hours of beam time were required to obtain a total of 372 $^{12}C_2$-$\alpha_2$ events. Data were accumulated at a current of about 0.7 $\mu$A of singly charged $^3$He beam. Although the targets had been shown to withstand about 1 $\mu$A of beam for longer than 4 h without deterioration, a new target spot was used every 4 h and the spectra were recorded at these intervals. Approximately half of the data was collected at $\theta_\alpha = 85.3°$ and $\theta_C = 62.7°$, and the other half was accumulated at $\theta_\alpha = 100.6°$ and $\theta_C = 50.6°$.

A partial singles main plus monitor detector spectrum, accumulated over 4 h at $\theta_\alpha = 85.3°$ (monitor detector at 94.7°), is shown in Fig. 3. Peaks labeled with (1) are from the monitor detector system and those labeled with (2) are from the main detector system. The $\alpha_2(2)$ peak is very clean and the typical peak to background ratio is 80 at the high energy side and 35 at the low energy side. The counts within the indicated 350 keV window were summed to give the number of singles $\alpha_2$ events ($N_\alpha$). The background was extrapolated linearly under the peak, and the uncertainty in $N_\alpha$ from all causes is estimated to be less than 0.5%.

Figure 4 shows a two-dimensional display of all the data taken at $\theta_\alpha = 85.3°$ and $\theta_C = 62.7°$. The number of coincidence events are displayed as a function of $^{12}$C recoil energy ($E_C$) and time-of-flight difference ($T$). Only events with an $\alpha$ energy ($E_\alpha$) within the energy window indicated in Fig. 3 are included. The $^{12}C_2$-$\alpha_2$ coincidence events of interest show up as a peak at $E_C$ channels 46 to 54 and $T$ channels 23 to 26. $^{12}C_2$ breakups produce the $^8$Be-$\alpha_2$ coincidence group at $E_C$ channels 50 to 54 and $T$ channels 16 to 19, and the strong ridge of $\alpha$-$\alpha_2$ coincidence events at low $E_C$ channels (the scale for the ridge is reduced by a factor of 20). The weak line occurring at $E_C$ channels 47 to 49 is from random coincidences with elas-

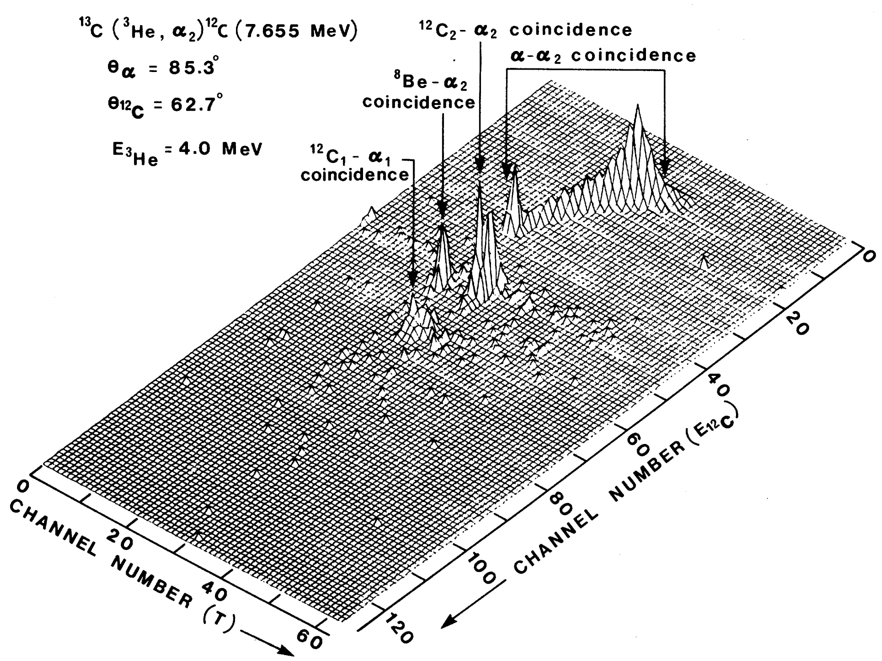


FIG. 4. Two dimensional display of partial coincidence events accumulated at $\theta_\alpha = 85.3°$ and $\theta_C = 62.7°$. Only events with an $\alpha$ energy within the window indicated in Fig. 3 are included.

tically scattered $^3$He, the most intense line in the singles spectrum for the $^{12}$C detector. The counts at $E_C$ channels 59 to 66 and $T$ channels 23 to 26 are $^{12}C_1$-$\alpha_1$ coincidence events which show up in this spectrum from the tail of the $\alpha_1$ peak.

Figure 5 shows the time spectrum obtained by summing the counts within $E_C$ channels 46 to 54 of the two-dimensional display in Fig. 4. The time calibration is 0.79 nsec/channel. The random coincidence rate between elastic $^3$He and $\alpha_2$ is rather low, contributing a correction of 3.4% over the four time channels indicated. No correction is necessary for data accumulated at $\theta_C = 50.6°$, as the $^3$He peak is well resolved from the $^{12}C_2$ peak at this angle.

Figure 6(a) shows a $^{12}$C spectrum obtained by summing the counts within the $T$ channels 23 to 26 of the two dimensional display in Fig. 4. The $^{12}$C line shape shown as a solid curve is obtained from $^{12}C_1$-$\alpha_1$ coincidence events, gated by the appropriate $\alpha_1$ group, and summed over appropriate $T$ channels. Figures 6(b) and 6(c) show $^{12}$C spectra obtained with a similar time window, but with windows in the $\alpha$ spectrum covering a 350 keV region on the high energy side [6(b)] and the low energy side [6(c)] of the $\alpha_2$ peak. For background subtraction, an average of the counts in Figs. 6(b) and 6(c) was used. The background correction amounts to 9.6% for data accumulated at $\theta_C = 62.7°$, and 11.3% for data accumulated at $\theta_C = 50.6°$. The energies of the background events in the $^{12}$C detector are shifted slightly as though following the kinematic line for a final state consisting of an $\alpha$ particle plus some nucleus with a mass near 12.

With the energy and time resolutions of the detector system, it is possible to impose the limit $9 \leq A_4 \leq 16$ on the masses of the heavy recoils that could possibly be confused with $^{12}C_2$ recoils. A kinematic search of reactions of the type $A_1$-($^3$He,$A_3$)$A_4$ with $7 \leq A_1 \leq 21$, $1 \leq A_3 \leq 4$, and all possible particle decays of $A_4$ has been done. The reaction $^{14}$N($^3$He, $\alpha_1$)$^{13}$N(2.37 MeV) and the subsequent $^{13}$N(2.37 MeV)$\rightarrow p + ^{12}$C decay give almost identical $\alpha$ and $^{12}$C energies to the $^{13}$C($^3$He, $\alpha_2$)-$^{12}$C reaction. No other reaction involving a known level in $A_4$ can produce events with the right $E_\alpha$, $E_C$, and $T$. However, reactions leading to some of the possible three-body final states can produce events with about the same energies and flight time difference. Such reactions would produce a smooth kinematic line in this region so that subtracting the average background in Figs. 6(b) and 6(c) from 6(a) would properly correct for this type of background. If the background came from "direct $\alpha$ capture" or "$\alpha$ capture" through the tails of wide resonances at higher excitation energies, the subtraction procedure would also remove these contributions.

The contribution from $^{13}$N (2.37 MeV) is estimated in the following manner. For the $^{12}$C solid angle used in our experiment, the proton decay of $^{13}$N (2.37 MeV) produces two $^{12}$C groups separated by 1 MeV in energy. They correspond to the proton being emitted along, or opposite to, the recoil direction. Since the spin of the $^{13}$N (2.37 MeV) level is $\frac{1}{2}$ (Ref. 16), the angular distribution of the protons is isotropic in the $^{13}$N center of mass system, and the relative yields of the two $^{12}$C recoil groups can be calculated. Figure 7 shows such a Monte Carlo calculation for $\theta_C = 62.7°$. The ratio

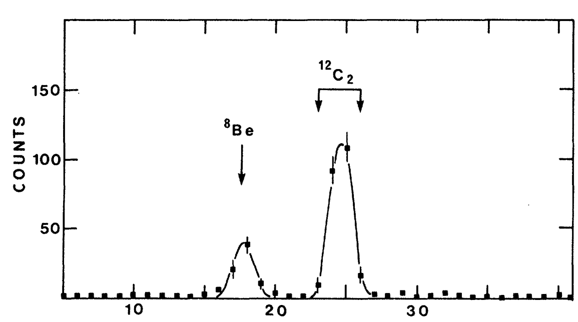


FIG. 5. Time spectrum obtained by summing over $E_C$ channels 46 to 54 of the two dimensional display in Fig. 4. The calibration is 0.79 nsec/channel.

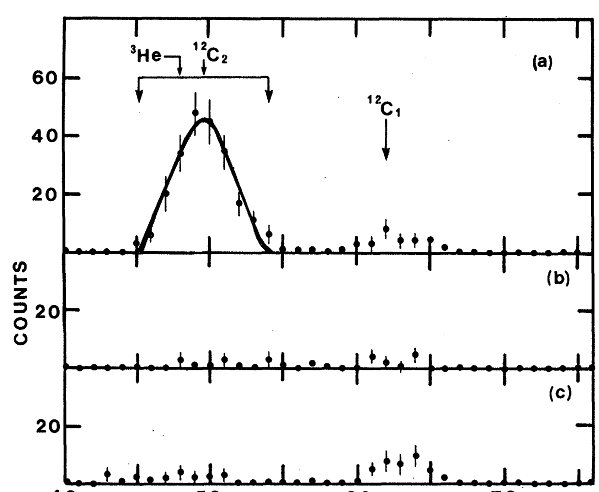


FIG. 6. (a) $^{12}$C spectrum obtained by summing over $T$ channels 23 to 26 of the two dimensional spectrum of Fig. 4. (b) Background $^{12}$C spectra obtained for a similar time window and a 350 keV window in the $\alpha$ detector on the high energy side and (c) the low energy side of the $\alpha_2$ peak.

$R$ of the number of higher energy recoils to the number of lower energy recoils is 1.53 at $\theta_C = 62.7°$ and 1.47 at $\theta_C = 50.6°$. The low energy $^{12}C$ group shows up weakly, but clearly, in the two dimensional displays of coincidence events as a function of $E_C$ and $T$. It is not visible in Fig. 4 because the group is quite close to the $\alpha$-$\alpha_2$ coincidence events and the scale there was suppressed. From the number of events in this lower energy $^{12}C$ group and the calculated ratio $R$, the $^{13}N$ (2.37 MeV) contribution is estimated to be 14.1% for data taken at $\theta_C = 62.7°$ and 15.9% for data taken at $\theta_C = 50.6°$. These corrections were consistent with results obtained from experiments carried out under almost identical arrangements, but with 15 times higher concentration of $^{14}N$ impurities.

Another check on the calculated values of $R$ is to calculate the effective solid angles subtended by the $^{12}C$ detector in the forward and backward directions in the $^{13}N$ (2.37 MeV) center of mass system. For $\theta_C = 62.7°$ the $^{12}C$ recoils could be detected by the $^{12}C$ detector if the proton is emitted within the angles $0° \leq \theta \leq 16°$ and $160.5° \leq \theta \leq 180°$ in the $^{13}N$ (2.37 MeV) center of mass system. Since the proton angular distribution has to be symmetric in the $^{13}N$ (2.37 MeV) center of mass coordinate, the ratio of the effective solid angle should give a good approximation to $R$. Such a calculation gives $R = 1.51$ at $\theta_C = 62.7°$ and $R = 1.45$ at $\theta_C = 50.6°$, which agrees quite well with results from Monte Carlo calculations. The estimated uncertainty in $R$ is about 10%.

The geometrical efficiency $\epsilon_2$ for detecting the $^{12}C_2$-$\alpha_2$ coincidence events was estimated from Monte Carlo calculations that closely reproduced the measured efficiencies $\epsilon_1$ and $\epsilon_0$ for detecting $^{12}C_1$-$\alpha_1$ and $^{12}C_0$-$\alpha_0$ coincidence events. Such calculations took into account the finite size of the beam spot, the offset of the detectors, multiple scattering from the target material (corrections were made for this small effect by using the parameters given by Marion and Young[17]), and the recoil effects due to the emission of $\gamma$ rays.

Calculation of the recoil effects required a knowledge of the angular distribution of $\gamma$ rays relative to the direction of emission of the $\alpha$ particles from the ($^3$He, $\alpha$) reaction. The angular distribution of the 4.44 MeV $\gamma$ rays from the first excited state of $^{12}C$, in coincidence with the $\alpha_1$ group, was found to be

$$W(\theta) = 1 - (0.52 \pm 0.10) P_2(\cos\theta) + (0.64 \pm 0.12) P_4(\cos\theta).$$

This deviation from isotropy resulted in a 1% change in the geometrical efficiency $\epsilon_1$.

For the second excited state ($J^\pi = 0^+$) the angular distribution of 3.22 MeV $\gamma$ rays is isotropic, and

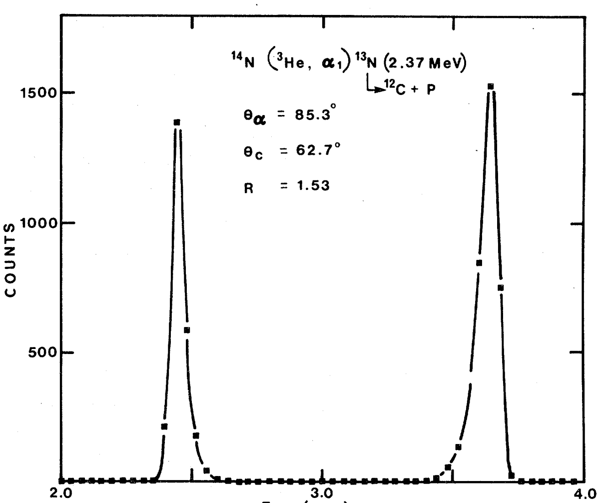


FIG. 7. Monte Carlo calculation of the $^{12}C$ spectrum from $^{13}N$ (2.37 MeV) breakup. The angular distribution of the proton was assumed to be isotropic in the $^{13}N$ center of mass system. The value $R$ is the ratio of the number of higher energy recoils to the number of lower energy recoils.

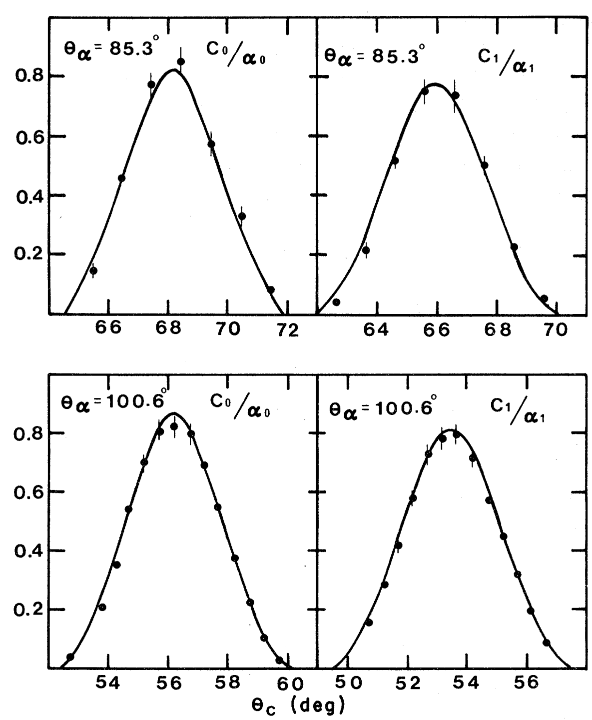


FIG. 8. Experimental geometrical efficiencies for detecting $^{12}C_1$–$\alpha_1$ and $^{12}C_0$–$\alpha_0$ coincidence events. The solid curves are efficiencies calculated by the Monte Carlo program.

TABLE I. A summary of the experimental results. $\theta_\alpha$ is the $\alpha$ detector angle, $\theta_C$ is the $^{12}$C detector angle, $N_\alpha$ is the number of singles $\alpha_2$ counts; $N_c$ is the number of $^{12}C_2$-$\alpha_2$ coincidence counts; and $\epsilon_2$ is the geometrical efficiency for detecting $^{12}C_2$-$\alpha_2$ coincidence events.

| $\theta_\alpha$ | $\theta_C$ | $N_\alpha$ | $N_c$ | $\epsilon_2$ | $\Gamma_{rad}/\Gamma$ |
|---|---|---|---|---|---|
| 85.3° | 62.7° | 344 524 ± 592 | 115 ± 13 | 0.73 ± 0.037 | $(4.57 \pm 0.58) \times 10^{-4}$ |
| 85.3° | 62.7° | 202 193 ± 465 | 62 ± 10 | 0.73 ± 0.037 | $(4.20 \pm 0.71) \times 10^{-4}$ |
| 100.6° | 50.6° | 377 114 ± 620 | 110 ± 13 | 0.78 ± 0.039 | $(3.74 \pm 0.48) \times 10^{-4}$ |
| 100.6° | 50.6° | 252 542 ± 507 | 85 ± 12 | 0.78 ± 0.039 | $(4.32 \pm 0.65) \times 10^{-4}$ |

the relative angular correlation of the subsequent 4.44 MeV $\gamma$ rays (from the $0^+ \to 2^+ \to 0^+$ cascade) was taken to be $(1 - 3\cos^2\theta + \cos^4\theta)$. No correction was made to allow for the positron-electron pair emission. Since $\Gamma_{e\pm}/\Gamma$ is about a factor of 70 smaller than $\Gamma_{rad}/\Gamma$, the error introduced is quite negligible.

Figure 8 shows the experimental $C_1$-$\alpha_1$ and $C_0$-$\alpha_0$ detection efficiencies as a function of $\theta_C$ at $\theta_\alpha = 85.3°$ and $\theta_\alpha = 100.6°$. The curves are the calculated efficiencies assuming a beam diameter of 1.19 mm as observed from the beam marks. Since the calculated curves fitted the data extremely well, the calculated efficiencies for detecting the $^{12}C_2$-$\alpha_2$ events were used in analyzing our data. The uncertainty in the calculated values of $\epsilon_2$ was estimated to be 5%, based on our ability to calculate the measured efficiencies $\epsilon_1$ and $\epsilon_0$.

The relative positions of the monitor detector and the $^{12}$C detector were chosen such that the geometrical efficiency for detecting the $^{12}C_0$-$\alpha_0$ coincidence events was about 55%. A small change in the beam position would significantly change this value, e.g. a change of 0.2° in the relative angles of the detectors would change the efficiency by 10%. The ratio was monitored throughout the experiment as a check on the stability of the experimental arrangement.

## IV. RESULTS AND CONCLUSIONS

The results of our measurements are listed in Table I. The uncertainties in the singles $\alpha_2$ counts ($N_\alpha$) and the coincidence counts ($N_c$) included uncertainties in counting statistics and background subtraction. The error in the weighted average took into account only uncertainties in $N_\alpha$ and $N_c$. The 5% uncertainty in geometrical efficiency was treated as a systematic error and combined with the resultant counting uncertainty in quadrature to give the quoted error. Our result $\Gamma_{rad}/\Gamma = (4.15 \pm 0.34) \times 10^{-4}$ agrees with the value $\Gamma_{rad}/\Gamma = (4.20 \pm 0.22) \times 10^{-4}$ published by Chamberlin *et al.*[3] and with the recently revised value $\Gamma_{rad}/\Gamma = (4.4 \pm 0.2) \times 10^{-4}$ of Davids *et al.*[18] This strongly suggests that the older accepted value[13] of $\Gamma_{rad}/\Gamma = (2.9 \pm 0.3) \times 10^{-4}$ may be too low.

Following the formalism of Fowler, Caughlan, and Zimmerman,[19] the reaction rate for the triple-$\alpha$ process can be written as

$$R = \frac{N_\alpha^3}{6 N_A^2} N_A^2 \langle \alpha\alpha\alpha \rangle , \qquad (5)$$

where $N_A$ is Avogadro's number, and $N_A^2 \langle \alpha\alpha\alpha \rangle$ is the quantity usually tabulated[19] and used to evaluate the stellar energy generation rate, or the mean lifetime for the destruction of helium by the triple-$\alpha$ process. Comparing Eqs. 4 and 5, the quantity $N_A^2 \langle \alpha\alpha\alpha \rangle$ is given by

$$N_A^2 \langle \alpha\alpha\alpha \rangle = 6 N_A^2 f_1 f_2 \frac{h^5 (3)^{3/2}}{(2\pi)^2 (M_\alpha K T)^3} \Gamma_{rad} \exp\left(-\frac{Q}{kT}\right) .$$

The weighted average of $\Gamma_{rad}/\Gamma$ from the latest three measurements is $\Gamma_{rad}/\Gamma = (4.24 \pm 0.15) \times 10^{-4}$. With the new values for $\Gamma_{rad}/\Gamma$ and $Q$ (Ref. 2), the quantity $N_A^2 \langle \alpha\alpha\alpha \rangle$ becomes

$$N_A^2 \langle \alpha\alpha\alpha \rangle = 2.95 \times 10^{-8} T_9^{-3} \times \exp(-4.4110/T_9) \mathrm{mole}^{-3} \mathrm{cm}^6 \mathrm{sec}^{-1} ,$$

where the electron screening factors $f_1$ and $f_2$ have been dropped, and $T_9$ is the temperature in $10^9$ K. Contributions from higher excited states of $^{12}$C are expected to be insignificant up to a temperature of about $7 \times 10^9$ K, and are ignored. The main source of error in $N_A^2 \langle \alpha\alpha\alpha \rangle$ is from the positron-electron branching ratio which has an uncertainty of 27%.

## ACKNOWLEDGMENTS

The authors would like to thank Mr. A. Mason for his work in different phases of the experiment, Mr. B. Cooke for his work on the related address program, Mr. M. Lukie for his help during the long runs, and especially Dr. C. N. Davids, Dr. C. A. Barnes, and Dr. R. N. Kavanagh for interesting and enlightening discussions. One of the authors (H.-B. Mak) would like to express his appreciation for the hospitality shown by Atomic Energy of Canada Limited while he was analyzing the data at the Chalk River Nuclear Laboratories

*Work supported by the Atomic Energy Control Board of Canada.

[1]C. A. Barnes and D. B. Nichols, Nucl. Phys. A217, 125 (1973).

[2]H. Stocker, A. A. Rollefson, and C. P. Browne, Phys. Rev. C 4, 1028 (1971); S. J. McCaslin, F. M. Mann, and R. W. Kavanagh, *ibid.* 7, 489 (1973); S. M. Austin, G. F. Trentleman, and K. Kashy, Astrophys. J. 163, 179 (1971); P. L. Jolivette, J. D. Goss, A. A. Rollefson, and C. P. Browne, Phys. Rev. C 10, 2629 (1974).

[3]D. Chamberlin, D. Bodansky, W. W. Jacobs, and D. L. Oberg, Phys. Rev. C 9, 69 (1974).

[4]E. J. Opik, Proc. R. Irish Acad. A54, 49 (1951).

[5]E. E. Salpeter, Astrophys. J. 115, 326 (1952).

[6]F. Hoyle, D. N. F. Dunbar, W. A. Wenzel, and W. Whaling, Phys. Rev. 92, 1095 (1953).

[7]C. W. Cook, W. A. Fowler, C. C. Lauritsen, and T. Lauritsen, Phys. Rev. 107, 508 (1957).

[8]D. D. Clayton, *Principles of Stellar Evolution and Nucleosynthesis* (McGraw-Hill, New York, 1968), p. 414.

[9]D. E. Alburger, Phys. Rev. 124, 193 (1961); I. Hall and N. W. Tanner, Nucl. Phys. 53, 673 (1964); P. A. Seeger and R. W. Kavanagh, *ibid.* 46, 557 (1963).

[10]H. Crannel, T. A. Griffy, L. R. Sulzle, and M. R. Yearian, Nucl. Phys. A90, 152 (1967).

[11]D. E. Alburger, Phys. Rev. 118, 235 (1960).

[12]A. W. Obst, T. B. Grandy, and J. L. Weil, Phys. Rev. C 5, 738 (1972).

[13]F. Ajzenberg-Selove and T. Lauritsen, Nucl. Phys. A114, 1 (1968).

[14]C. N. Davids, R. C. Pardo, and A. W. Obst, Bull. Am. Phys. Soc. 19, 556 (1974); R. G. Markhan, S. M. Austin, and M. A. M. Shahabuddin, *ibid.* 19, 1003 (1974); A. W. Obst, W. J. Braithwaite, and C. H. King, *ibid.* 19, 1003 (1974).

[15]H.-B. Mak, H. C. Evans, G. T. Ewan, A. B. McDonald, and T. K. Alexander, Bull. Am. Phys. Soc. 20, 31 (1975).

[16]H. L. Jackson and A. I. Galonsky, Phys. Rev. 89, 370 (1953); E. A. Milne, *ibid.* 93, 762 (1954).

[17]J. B. Marion and F. C. Young, *Nuclear Reaction Analysis* (North-Holland, Amsterdam, 1968), p. 30.

[18]C. N. Davids, R. C. Pardo, and A. W. Obst (private communication).

[19]W. A. Fowler, G. R. Caughlan, and B. A. Zimmerman, Annu. Rev. Astron. Astrophys. 5, 525 (1967); *ibid.* (to be published).